Engineering Chemistry
ISSN: 2813-6535, Vol. 1, pp 39-44
doi:10.4028/p-489m23
© 2023 The Author(s). Published by Trans Tech Publications Ltd, Switzerland.
Submitted: 2022-12-12
Accepted: 2022-12-28
Online: 2023-03-30

Peak Wavelength Mapping of Triangular Reflection in Spherical Colloidal Cluster with Icosahedral Symmetry

Ryosuke Ohnuki[1,a,*], Yukikazu Takeoka[2,b] and Shinya Yoshioka[1,c]

[1]Graduate School of Science and Technology, Tokyo University of Science, Yamazaki, Noda 278-8510, Japan

[2]Graduate School of Engineering, Nagoya University, Furo-cho, Chikusa-ku, Nagoya 464-8603, Japan

[a]6220701@ed.tus.ac.jp, [b]ytakeoka@chembio.nagoya-u.ac.jp, [c]syoshi@rs.tus.ac.jp

Keywords: Colloidal cluster, Structural color, Icosahedral symmetry

Abstract. Spherical colloidal clusters have various types of particle arrangements. Interestingly, one type has an icosahedron symmetry, characterized by the existence of five-fold axes. When the colloidal particle size is comparable to the wavelength of light, icosahedral colloidal clusters exhibit a unique triangular reflection with a specific wavelength, owing to optical interference. In this paper, we report the results of a detailed optical study on the position-dependent peak wavelength within the triangular region. Based on the map of the peak wavelength and spectral shape, we propose a structural model of the icosahedral colloidal cluster and discuss its formation process.

Introduction

Colloidal clusters with spherical shapes can be easily produced from water-in-oil-type emulsions by evaporating water [1,2]. When the size of colloidal particles is comparable to the wavelength of light, the clusters produce brilliant structural colors because of the interference of light. Thus, colloidal clusters have been widely applied in optical materials, such as colorimetric sensors [3-8] and pigments [9-11]. It was recently discovered that spherical colloidal clusters have different particle arrangements depending on the preparation conditions, for example, the number of particles inside micelles and the shrinking speed of micelles. These types include clusters with icosahedral symmetry [12-19], decahedral symmetry [18,19], and an onion-like structure in which layers of the arranged particles are stacked beneath the sphere surface [1,2,20-22].

We were particularly interested in the icosahedral type. The particle arrangement is characterized by six five-fold axes, which are incompatible with the translational symmetry of the seven crystal system types. In our previous study, we performed an optical investigation of a large icosahedral colloidal cluster [14]. A unique triangular reflection appears on the spherical cluster surface, corresponding to one of the 20 triangles of the icosahedron; when the sample is rotated, a different triangle is reflected under an optical microscope [14,19].

It has been presumed that spherical colloidal clusters with icosahedral symmetry consist of 20 Mackay tetrahedra [23] as shown in Fig. 1(a). The Mackay tetrahedron has a slightly deformed shape, different from that of a regular tetrahedron. One of the four triangles is larger than the others, and this large triangle faces the outside of the colloidal cluster (Fig. 1(b)). The reflected wavelength is sensitive to the distance between the colloidal particle layers. We previously reported that the reflectance spectrum of the triangular reflection has a large peak, and the peak position is reasonably consistent with the wavelength calculated from the Bragg condition, assuming the particle arrangement of the Mackay tetrahedron [14]. However, a thorough inspection revealed that the experimental peak wavelength was slightly longer than the theoretically calculated wavelength. In addition, the peak shape was not observed to be symmetrical but appeared as an additional component at a wavelength longer than the peak [14]. Thus, we further investigated the triangular reflection.

In this study, we investigated the variation in the peak wavelength with the position within the triangular reflection. Reflectance spectra were measured at many positions using microspectroscopy,

This article is an open access article under the terms and conditions of the Creative Commons Attribution (CC BY) license (https://creativecommons.org/licenses/by/4.0)

and the peak wavelength was mapped. From the resultant map, we propose a modified particle arrangement of a large icosahedral cluster consistent with the observed optical properties.

Method

Preparation of Spherical Colloid Clusters. The icosahedral colloidal cluster used in this study was the same as that used in our previous study [14]. A summary of the preparation method is presented as follows: a suspension containing 310 nm colloidal particles at a concentration of 5 v/v% and hexadecane containing 2 wt% Span80 was prepared. Hexadecane was presaturated with water to slow down the droplet evaporation. Next, droplets of the suspension in hexadecane, that is, W/O emulsion, were prepared, and the water was slowly evaporated at room temperature (approximately 20 °C). Finally, after "three weeks", the samples were washed several times with hexane and dried at room temperature.

Microspectroscopy. To measure the reflectance spectrum of a small region within the triangular reflection of clusters with icosahedral symmetry, we applied microspectroscopy using an optical microscope (Olympus BX51). A xenon lamp was used as the light source, and a 100× objective lens (Olympus, SLMPlan N N.A.= 0.60) was used for observation. An optical fiber with a diameter of 200 µm was placed at the imaging position of the microscope to direct the reflected light from the microscopic region to the spectrometer (Ocean Optics, USB2000). The measurement area was a spot with a diameter of 200/100 = 2 µm. Reflectance was calculated as the ratio of the reflection of the sample to that of a diffused reflection standard (Labsphere Spectralon).

Results and Discussion

A spherical colloidal cluster with icosahedral symmetry can be modeled by combining 20 Mackay tetrahedra, slightly distorted from a regular tetrahedron, as shown in Fig. 1. The icosahedron was truncated to a spherical shape to obtain a realistic model of the colloidal cluster [15,23]. The direction from the center of the icosahedron to the surface triangle center corresponds to the [111] direction of the face-centered cubic (FCC) lattice (Fig. 1(b)). Although the particle arrangement is not exactly the FCC lattice in the Mackay tetrahedron owing to the deformation, the Millar index [111] is often used to refer to the direction because the particle arrangement is hexagonal in the plane of the surface triangle (Fig. 1). The calculated height in this direction was 0.795 when the distance from the center

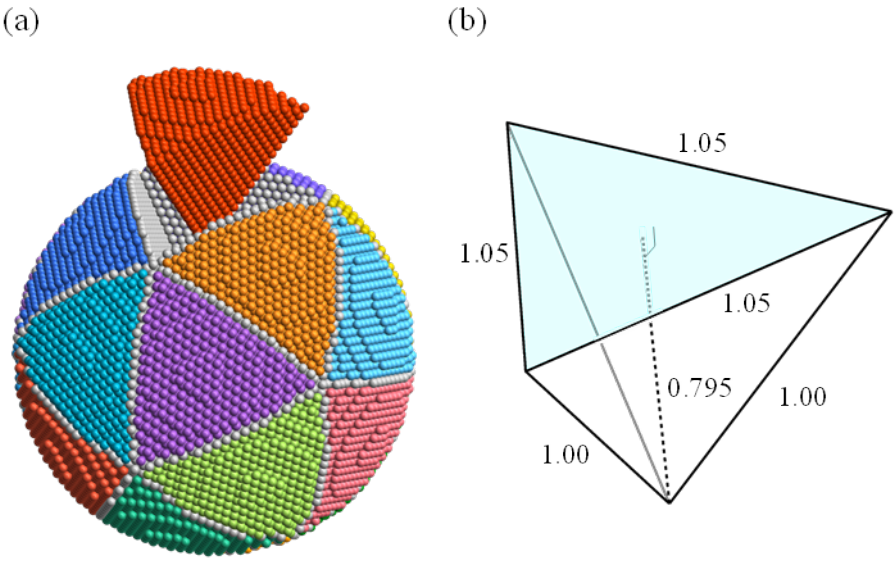

Figure 1. Model structure of spherical colloidal cluster with icosahedral symmetry. The cluster consists of 20 Mackay tetrahedra, and each Mackay structure is color-coded for identification. One Mackay structure is shifted upward (red grain). (b) Ratio of side and height of Mackay tetrahedron. The light-blue triangle corresponds to the icosahedron surface, of which lengths of the three sides are 1.05 each when the other sides have a length of 1.00. The height of the Mackay tetrahedron is 0.795, defined as the length between the center of the blue triangle and the other vertex.

of the icosahedron to the vertices on the surface was 1.00. From this length, the plane distance in the [111] direction of the Mackay tetrahedron, d_{M}, is expressed as

$$d_{\mathrm{M}} = 0.795 \times D, \tag{1}$$

where D is the diameter of the colloidal particles, as the colloidal particles were arranged at the tetrahedron vertices. Based on the size of the colloidal particles used in this study, $D = 310$ nm, and Eq. (1), the plane distance is $d_{\mathrm{M}} = 246$ nm. The mean refractive index, n_{M}, of the icosahedral cluster was estimated as

$$n_{\mathrm{M}} = n_{\mathrm{s}} f_{\mathrm{M}} + n_{\mathrm{a}}(1 - f_{\mathrm{M}}), \tag{2}$$

where n_{s} and n_{a} are the refractive indices of silica and air, respectively, and f_{M} is the volume fraction of the Mackay structure. When the refractive indices of silica and air are $n_{\mathrm{s}} = 1.46$ and $n_{\mathrm{s}} = 1.00$, respectively, and the volume fraction is $f_{\mathrm{M}} = 0.69$ [23], the mean refractive index is $n_{\mathrm{M}} = 1.32$ from Eq. (2). The wavelength of the reflected light from this direction is expected from the Bragg condition to be

$$\lambda_{\mathrm{M}} = 2 n_{\mathrm{M}} d_{\mathrm{M}} \cos\theta, \tag{3}$$

where θ is the incidence angle on the (111) plane. Substituting the values of d_{M} and n_{M} and $\theta = 0°$ into Eq. (3) yields $\lambda_{\mathrm{M}} = 649$ nm.

Keeping this wavelength in mind, we measured the reflectance spectrum at many positions inside the triangular reflection, as shown in Fig. 2(a). For example, the reflectance spectrum near the center of the triangular reflection is shown in Fig. 2(b). The spectrum at most positions shows a large peak with a few small side peaks, and the peak wavelength ranges from approximately 650 to 700 nm. Fig. 2(c) shows the color map obtained from the wavelength of the main reflectance peak.

At all the measurement positions, the experimentally determined wavelength was longer than the calculated value of 649 nm. In addition, the wavelength was longer at the center of the triangle than near the edge, as shown in Fig. 2(c). A possible reason for this variation is the difference in the incidence angle to the (111) plane, as the Bragg condition includes the cosine factor. However, quantitative analysis shows that this effect does not sufficiently explain the wavelength variation. The incident angle to the spherical surface at the edge of the triangle was approximately 20°, which could be estimated from the structural model (Fig. 1(a)). When refraction at the surface is considered using the mean refractive index, it is expected that the incident angle to the (111) plane becomes approximately 15°. The wavelength under the Bragg condition calculated using this angle was

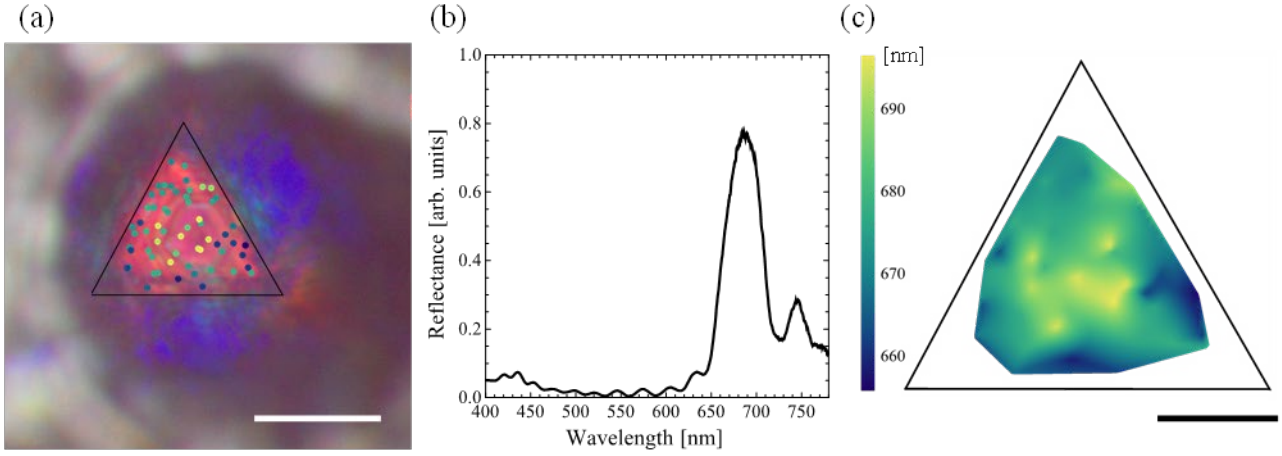

Figure 2. Measurement positions in triangular reflection. The color of the small filled circle at the measurement position indicates the peak wavelength, which corresponds to the color scale in (c). The scale bar is 10 μm. (b) Typical reflectance spectrum around center of triangular reflection. (c) Map of peak wavelength in triangular region. The scale bar is 5 μm.

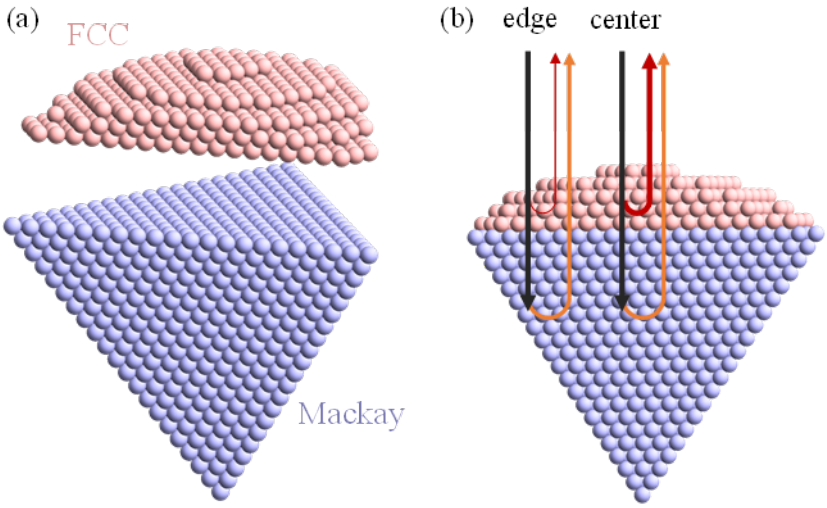

Figure 3. (a) Model of unit structure composed of spherical colloidal cluster with icosahedral symmetry. The inner part of the cluster has the Mackay structure, with the FCC structure on surface part. (b) Schematic of difference in reflectance at different positions of triangular region. Reflections from the FCC structure are indicated by red arrows, and those from the Mackay structure are indicated by orange arrows. The thickness of the arrows indicates the reflection intensity.

approximately 20 nm shorter than the wavelength under normal incidence. However, the experimentally observed shift was approximately 50 nm, more than twice the shift expected from a tilted incidence.

We heuristically consider the FCC lattice to explain why the observed peak wavelength is longer than the theoretical wavelength calculated using Eq. (3). Because the Mackay tetrahedron has a shape compressed from the regular tetrahedron in the height direction (Fig. 1(b)), the plane distance d_{M} is shorter than that of the non-deformed FCC lattice. The plane distance in the [111] direction of the FCC lattice, d_{F}, is expressed as

$$d_{\mathrm{F}} = \frac{\sqrt{6}}{3} \times D. \tag{4}$$

From $D = 310$ nm and Eq. (4), the plane distance is $d_{\mathrm{F}} = 253$ nm. The mean refractive index, n_{F}, of the FCC lattice was estimated as

$$n_{\mathrm{F}} = n_{\mathrm{s}} f_{\mathrm{F}} + n_{\mathrm{a}}(1 - f_{\mathrm{F}}), \tag{5}$$

where f_{F} is the volume fraction of the FCC lattice. Using a volume fraction $f_{\mathrm{F}} = 0.74$, the mean refractive index is $n_{\mathrm{F}} = 1.34$ from Eq. (5). The wavelength λ_{F} from the (111) planes of the FCC lattice was calculated from the Bragg condition as

$$\lambda_{\mathrm{F}} = 2 n_{\mathrm{F}} d_{\mathrm{F}} \cos\theta. \tag{6}$$

Substituting the values of d_{F} and n_{F} and $\theta = 0°$ into Eq. (6) yields $\lambda_{\mathrm{F}} = 678$ nm. This wavelength is approximately 30 nm longer than the wavelength, λ_{M}, calculated for the Mackay structure, which may explain the longer experimentally observed wavelength.

From the above calculation of λ_{F} and the plotted color map shown in Fig. 2, we developed a model structure (Fig. 3). In this model, 20 Mackay tetrahedra form the core of the spherical cluster, and particle arrangements of the FCC lattice occur near the surface. The surface FCC lattice has a different number of colloidal particle layers depending on the position because of the spherical shape of the clusters: the number of layers is higher in the center of the triangle and smaller near the edge.

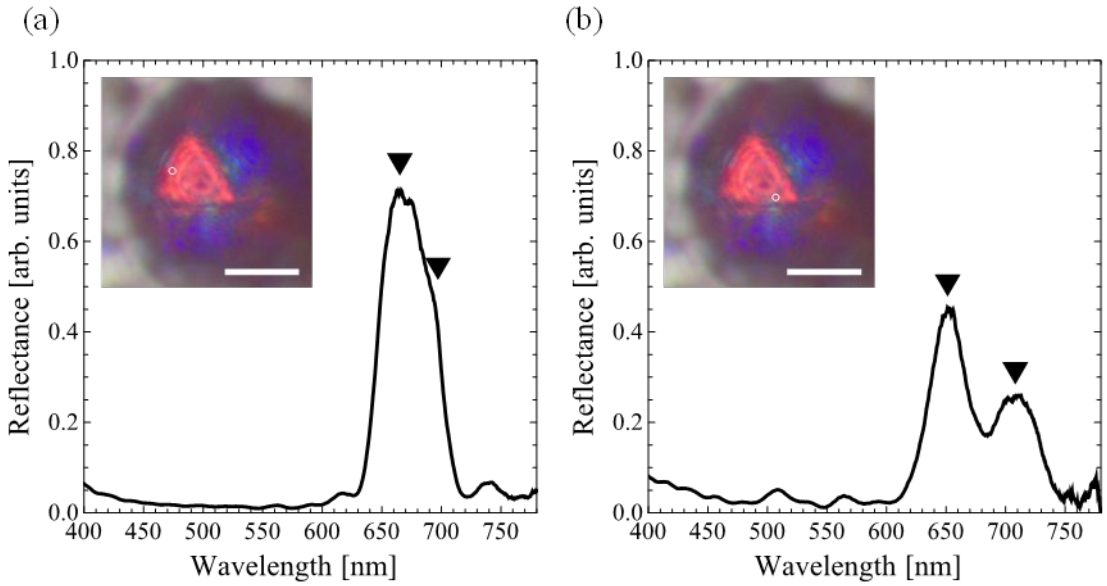

Figure 4. Reflectance spectra in the triangular region. (a) Example of a reflection peak with a shoulder and (b) example of two reflection peaks. The inset image is an optical micrograph indicating the measurement position (white circle). The scale bar is 10 μm.

This difference affects the magnitude of reflectance at wavelength λ_F. Thicker FCC layers result in higher reflectance, whereas a lower reflectance is expected near the edge (Fig. 3(b)). This model expects two contributions in the reflectance spectrum originating from Mackay and FCC structures. The different magnitudes of the contributions explain the variation in the peak wavelength of the triangular reflection because, at the edge of the triangle, the reflection from the Mackay tetrahedron is thought to be dominant at wavelength λ_M.

Fig. 4 shows examples of the spectra that support the hypothetical model above. Fig. 4(a) shows the reflectance spectrum observed near the edge of the triangle, which has a peak located at a wavelength close to wavelength λ_M calculated from the Mackay structure. However, in-depth examination reveals that there appears to be a spectral component at approximately 690 nm as a shoulder, which can be attributed to reflections from the FCC structure. Fig. 4(b) shows another spectrum observed at a different position, where the two reflection peaks are observed separately. In this case, the wavelength of the largest peak was used for mapping.

The model structure shown in Fig. 3 is still hypothetical; thus, further investigation is required. Although the particle arrangement is expected to be incommensurate in the interfacial plane between the Mackay and FCC structures, this model may be supported by previous studies on the process of colloidal cluster formation. It has been experimentally observed that crystallization commences at the water droplet surface [24]. Based on computer simulations, crystallization is also expected to occur in the interior of the droplet [13,15,25] when the droplet shrinks and the filling fraction of particles increases to approximately 0.50. Correspondingly, Chen *et al*. reported that a mismatch in the lattice constant occurs in the interior and surface parts of a cluster [26]. Therefore, the peak wavelength variation observed in this study might indicate that the cluster formation is a competition between the FCC lattice crystallization from the surface and the Mackay structure formation in the interior.

Summary and Conclusion

In conclusion, we investigated triangular reflection in spherical colloidal clusters with icosahedral symmetry by mapping the wavelength of the peak reflectance. The peak wavelength distribution and reflectance spectra shape were interpreted using a model structure combining the Mackay tetrahedron and FCC lattice. This model is consistent with those of previous studies on the formation mechanism of spherical colloidal clusters. The results of this study are expected to provide a clue to the formation process of spherical colloidal clusters into the icosahedral structure.

Acknowledgment

This study was supported by JSPS KAKENHI (Grant Number 22J12152).

References

[1] Y. Zhao, L. Shang, Y. Cheng and Z. Gu: Acc. Chem. Res. Vol. 47 (2014), p. 3632

[2] N. Vogel, S. Utech, G. T. England, T. Shirman, K. R. Phillips, N. Koay, I. B. Burgess,M. Kolle, D. A. Weitz and J. Aizenberg: Proc. Natl. Acad. Sci. U.S.A. Vol. 112 (2015), p. 10845.

[3] T. M. Choi, K. Je, J.-G. Park, G. H. Lee and S.-H. Kim: Adv. Mater. Vol. 30 (2018), p. 1803387

[4] G. Isapour and M. Lattuada: ACS Appl. Nano Mater. Vol. 4 (2021), p. 3389

[5] G. Isapour, B. H. Miller and M. Kolle: Adv. Photonics Res. Vol. 3 (2022), p. 2100043

[6] W. Luo, J. Yan, Y. Tan, H. Ma and J. Guan: Nanoscale Vol. 9 (2017), p. 9548

[7] Y. Ohtsuka, M. Sakai, T. Seki, R. Ohnuki, S. Yoshioka and Y. Takeoka: ACS Appl. Mater. & Interfaces Vol. 12 (2020), p. 54127

[8] Z. Yu, C.-F. Wang, L. Ling, L. Chen and S. Chen: Angew. Chem. Vol. 124 (2012), p. 2425

[9] S. H. Han, Y. H. Choi and S.-H. Kim: Small Vol. 18 (2022), p. 2106048

[10] R. Ohnuki, M. Sakai, Y. Takeoka and S. Yoshioka: Langmuir Vol. 36 (2020), p. 5579

[11] M. Sakai, T. Seki and Y. Takeoka: Small Vol. 14 (2018), p. 1800817

[12] C. Kim, K. Jung, J. W. Yu, S. Park, S.-H. Kim, W. B. Lee, H. Hwang, V. N. Manoharan and J. H. Moon: Chem. Mater. Vol. 32 (2020), p. 9704

[13] B. De Nijs, S. Dussi, F. Smallenburg, J. D. Meeldijk, D. J. Groenendijk, L. Filion, A. Imhof, A. Van Blaaderen and M. Dijkstra: Nat. Mater. Vol. 14 (2015), p. 56

[14] R. Ohnuki, N. Kunimoto, Y. Takeoka and S. Yoshioka: Part. Part. Syst. Charact. Vol. 39 (2022), p. 2100257

[15] J. Wang, C. F. Mbah, T. Przybilla, B. A. Zubiri, E. Spiecker, M. Engel and N. Vogel: Nat. Commun. Vol. 9 (2018), p. 5259

[16] J. Wang, C. F. Mbah, T. Przybilla, S. Englisch, E. Spiecker, M. Engel and N. Vogel: ACS Nano Vol. 13 (2019), p. 9005

[17] W. Wu, L. Wang, Y. Wang, L. Guo, S. Dong and J. Hao: J. Colloid Interface Sci. Vol. 563 (2020), p. 308

[18] S. Park, H. Hwang, M. Kim, J. H. Moon and S.-H. Kim: Nanoscale Vol. 12 (2020), p. 18576

[19] J. Wang, U. Sultan, E. S. Goerlitzer, C. F. Mbah, M. Engel and N. Vogel: Adv. Funct. Mater. Vol. 30 (2020), p. 1907730

[20] S.-H. Kim, J.-G. Park, T. M. Choi, V. N. Manoharan and D. A. Weitz: Nat. Commun. Vol. 5 (2014), p. 3068

[21] R. Ohnuki, S. Isoda, M. Sakai, Y. Takeoka and S. Yoshioka: Adv. Opt. Mater. Vol. 7 (2019), p. 1900227

[22] R. Ohnuki, M. Sakai, Y. Takeoka and S. Yoshioka: Adv. Photonics Res. Vol. 2 (2021), p. 2100131

[23] A. L. Mackay: Acta Crystallogr. Vol. 15 (1962), p. 916

[24] T. M. Choi, G. H. Lee, Y.-S. Kim, J.-G. Park, H. Hwang and S.-H. Kim: Adv. Mater. Vol. 31 (2019), p. 1900693

[25] F. Montanarella, J. J. Geuchies, T. Dasgupta, P. T. Prins, C. Van Overbeek, R. Dattani, P. Baesjou, M. Dijkstra, A. V. Petukhov, A. Van Blaaderen, *et al.*: Nano Lett. Vol. 18 (2018), p. 3675

[26] Y. Chen, Z. Yao, S. Tang, H. Tong, T. Yanagishima, H. Tanaka and P. Tan: Nat. Phys. Vol. 17 (2021), p. 121